Assignment 2 - Segmentation of a Vision Dataset

Problem Statement

In computer vision, precisely identifying and delineating specific areas within images, such as those containing pets like cats and dogs, presents a complex challenge that has garnered significant attention. This endeavor is not just a theoretical exercise. Still, it carries substantial relevance, especially in applications like automated content moderation, enhanced search functionalities within digital photo libraries, and even in the development of intelligent systems capable of interactive responses based on visual cues. The crux of the problem lies in creating an algorithm that can accurately segment parts of an image where a cat or dog is present without necessarily distinguishing between the two. This specificity is crucial for applications where the mere presence of a pet is the required information, irrespective of its species.

Addressing this challenge necessitates a solution capable of understanding and processing the intricate patterns and diverse features inherent in images of cats and dogs. These features can vary widely due to differences in size, color, pose, and even the environment in which the pet is situated. The U-NET architecture, renowned for its efficacy in medical image segmentation, is proposed as the foundation for the model due to its unique design that enhances the capture of contextual information at various resolutions. This architecture employs a symmetric expanding path that enables precise localization, making it particularly suitable for the task.

The justification for adopting a deep learning (DL) approach, specifically the U-NET architecture, for this segmentation task, is manifold. Firstly, DL models, by their very nature, excel at learning hierarchical feature representations from large datasets, making them adept at handling the high variability in images containing cats and dogs. This capability is paramount in segmentation tasks where the distinction between the subject and the background can be nuanced. Secondly, the convolutional layers in U-NET allow for capturing spatial hierarchies in images, which is critical for understanding the complex shapes and textures associated with pets. Additionally, the skip connections within U-NET facilitate the blending of low-level detail with high-level semantic information, ensuring that the segmented output retains the accuracy of the overall shape and the finer details, often lost in deeper networks.

Furthermore, the task transcends traditional object detection or classification because it focuses on pixel-wise segmentation. This level of granularity requires a model that not only recognizes the presence of a cat or dog but also delineates every pixel belonging to the pet from the rest of the image. Such precision demands the robust feature extraction and spatial encoding capabilities inherent in DL models, particularly those designed for segmentation tasks like U-NET.

In conclusion, developing a model based on the U-NET architecture for segmenting images to identify areas containing cats or dogs without differentiating between them addresses a

significant problem with wide-ranging applications. The choice of a DL solution, particularly U-NET, is justified by the need for a system capable of managing the high variability and complexity associated with pet images and the requirement for precise, pixel-level segmentation. This approach promises to advance the field of computer vision and offers practical solutions to real-world problems where understanding the visual context is paramount.

Data

The dataset in consideration serves as the cornerstone for developing a model aimed at image segmentation, specifically designed to isolate areas containing cats or dogs within a given image. This dataset is meticulously structured into a training set with 3,680 examples and a test set comprising 3,669 examples, thereby providing a substantial volume of data crucial for effectively training and validating a deep learning model. The dataset possesses a multifaceted FeaturesDict, including file names, images, labels, segmentation masks, and species classifications, catering to a comprehensive analytical approach toward image segmentation.

During the exploratory data analysis, it became evident that the images and their corresponding segmentation masks are consistently resized to a dimension of 128x128 pixels. This uniformity in size ensures that the model receives standardized input, essential for maintaining consistency in feature detection and segmentation performance. The images are in full color (RGB), encoded in 3 channels, and the segmentation masks are single-channel grayscale images where the pixel intensity denotes the presence of a cat or dog within the corresponding pixel in the source image. This binary nature of the masks aligns perfectly with the objective of the segmentation task, which is to distinguish the target areas (where pets are present) from the background.

The consistency and clarity in the feature structure of the dataset are commendable. It avoids unnecessary complexity while providing all the critical elements required for a deep learning model to learn the nuances of image segmentation. Including a segmentation mask for each image is particularly noteworthy as it offers a precise ground truth for the model to aim for during the training process.

Given that the dataset is originally sourced from the respected 'Cats and Dogs' collection, as cited, it indicates a rich diversity in the visual representation of the subjects, which is crucial for the generalization capability of the segmentation model. This diversity encompasses variations in poses, sizes, breeds, and backgrounds. The preprocessing step of resizing the images and masks to 128x128 ensures that the dataset is optimized for computational efficiency while retaining sufficient resolution to capture the necessary features for accurate segmentation.

The described dataset is robust, well-structured, and adequately preprocessed. It is highly suitable for training a U-NET-based deep learning model for segmenting images to identify regions containing a cat or dog. The data's composition allows for sophisticated model training that can discern and delineate the complex patterns of pet presence within various contexts,

thereby underlining this dataset's significance and potential in advancing the capabilities of image segmentation models.

Preprocessing

The preprocessing and augmentation of the dataset are critical steps in preparing the input data for the model, particularly for a task as delicate as image segmentation. These steps aim to diversify the training examples and help the model generalize better to unseen data by simulating various conditions that could occur in real-world scenarios. In this case, the preprocessing pipeline has been streamlined to utilize only the images and their corresponding segmentation masks, omitting all other features from the original dataset to maintain focus on the segmentation task.

During preprocessing, images and masks undergo augmentation to enhance the dataset's diversity and robustness. The augmentation includes a conditional operation where images and masks are flipped horizontally with a probability of 50%. This stochastic flipping introduces a level of variation that mimics the natural occurrence of pets in varying orientations, thereby enabling the model to learn and predict segmentation maps independent of the initial orientation of the subject within the image.

In addition to flipping, the images are subjected to random brightness adjustments, with a maximum delta of 0.2. This alteration simulates different lighting conditions, ensuring the model's robustness against variations in illumination that can significantly impact the appearance and visibility of features in an image.

The dataset has been split using a stratified approach further to strengthen the model's training and validation process. 80% of the training data is utilized for the actual training process, while the remaining 20% serves as a validation set. This separation ensures that the model is evaluated on its ability to memorize the training data and its capacity to generalize to new, similar data. Such a split is instrumental in fine-tuning the model parameters. It helps in the early detection of overfitting, where the model performs well on the training data but poorly on unseen data.

Removing other dataset features, such as file names, labels, and species information, which are not essential for the segmentation task, indicates a deliberate choice to streamline the dataset and focus the model's learning capabilities on the critical segmentation task. This minimization of input features helps reduce potential noise and distractions, enabling the model to concentrate on learning the key patterns and attributes relevant to the segmentation process.

Model

The tuning process for the segmentation model was managed by leveraging a hyperparameter tuner, which systematically explored the hyperparameter space to optimize the model's performance. This tuner was configured to execute 20 trials, each evaluating a unique set of hyperparameters. The tuner's configuration, designed to balance computational efficiency with thorough exploration, was set to run a maximum of four trials, each with a single execution, over 20 epochs. It employed early stopping with the patience of three epochs to prevent overfitting and expedite the search by halting the training if the validation loss failed to improve. A multiplier of five was utilized, likely influencing the scaling of other hyperparameters or model dimensions during the tuning process.

Hyperparameter tuning is a systematic process where each potential model's performance is evaluated, and the best-performing hyperparameters are selected. In this scenario, the tuner varied two primary hyperparameters: the number of blocks in the U-NET architecture and the initial number of filters in the convolutional layers. The 'num_blocks' hyperparameter was allowed to range from 2 to 4, incrementing by one, which dictated the depth of the U-NET architecture. The 'initial_num_filters' hyperparameter could range from 32 to 128 in steps of 32, determining the complexity and learning capacity of the initial convolutional layer. This thoughtful configuration allowed the tuner to evaluate models ranging from less complex and computationally light to more complicated and potentially more expressive.

As per the chosen hyperparameters, the final model exhibited four blocks, each comprising a sequence of layers, including a convolutional layer followed by batch normalization and ReLU activation, repeated twice per block. This pattern provides the feature extraction capabilities inherent to convolutional layers and introduces batch normalization and non-linearity, essential components for effectively training deep learning models. The final model also started with a minimum of 32 filters, progressively getting bigger to 64, 128, and 256 after every max pooling. You can see a visualization of the entire model in the main.ipynb file (the image is too big for a pdf).

The model adhered to the typical U-NET pattern, with each block's final convolutional layer undergoing max pooling with a 2x2 kernel to reduce spatial dimensions, effectively doubling the number of filters in subsequent blocks, thus expanding the model's capacity to capture increasingly abstract features at lower resolutions. Concomitantly, the 'decoder' part of the architecture received the output from the corresponding 'encoder' block, enabling the network to leverage high-level and low-level features for precise segmentation.

For the output layer, a 1x1 convolution was applied with three filters, each corresponding to a class, and a 'softmax' activation function, enabling the model to output a probability distribution over the classes for each pixel, a standard approach for multi-class segmentation tasks.

The chosen mode was subject to further training for 100 epochs. An EarlyStopping callback was employed, monitoring the validation loss with patience of 15 epochs to cease training if no improvement was observed, enhancing computational efficiency and preventing overfitting. The model concluded its training early at epoch 55, indicating it reached an optimal state according to the tuner's criteria before completing the pre-set number of epochs.

This sophisticated application of hyperparameter tuning exemplifies a structured approach to model optimization, with the tuner serving as an automated guide, steering the model development through the vast hyperparameter space to identify the most effective configuration for the task at hand.

Figures/Results

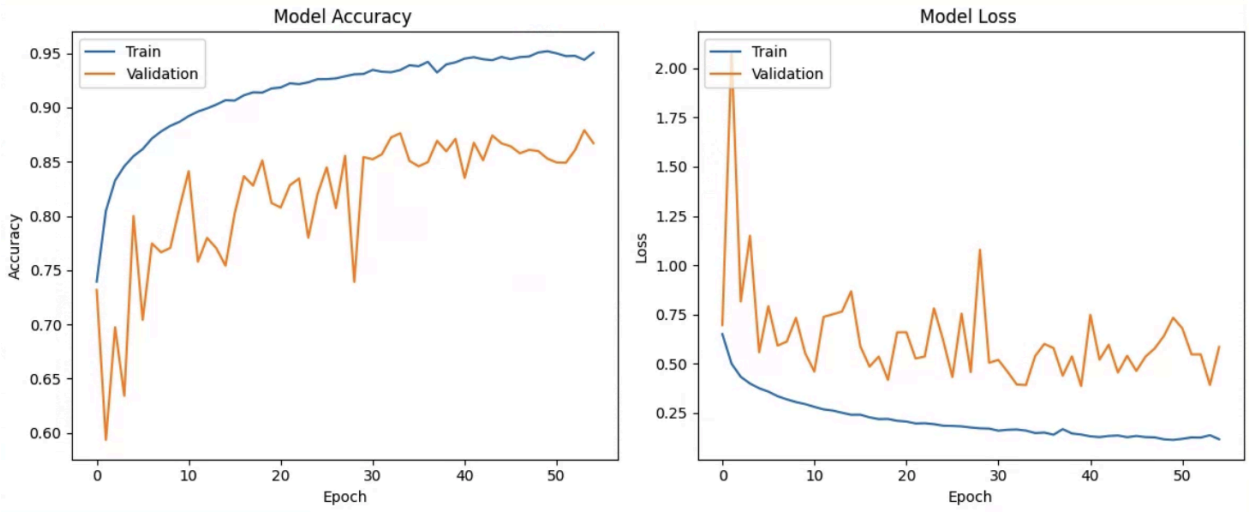

As shown in the graphs, the "Model Accuracy" graph indicates that training accuracy improved consistently over time, starting from a lower point and reaching a final accuracy of approximately 95.06%. In contrast, the validation accuracy exhibits more fluctuations throughout the training process, concluding at a final value of 86.71%. The "Model Loss" graph presents a declining trend for training loss, beginning at a higher value and descending to a final loss of 0.1162. The validation loss decreases initially but with noticeable variability across epochs, resulting in a final value of 0.5849. Both graphs display the model's performance over 55 epochs, after which an early stopping mechanism halted the training. The provided data points indicate the final training and validation losses and accuracies for the model at the cessation of training. The final training and validation metrics were loss: 0.1162 - Accuracy: 95.06% for training and val_loss: 0.5849 - val_accuracy: 86.71% for validation.

Best Predictions

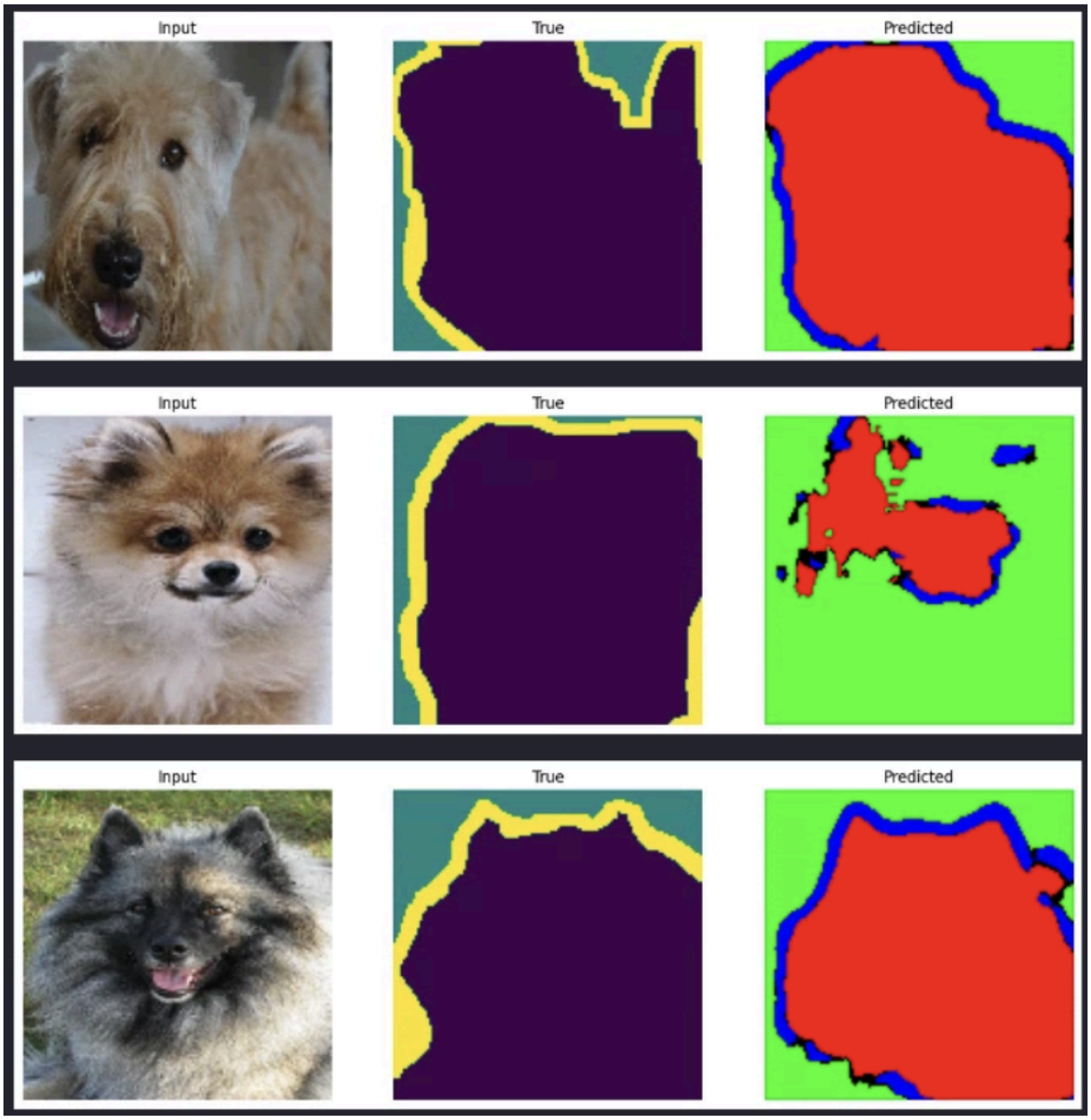

Worst Predictions

In examining the model's performance through the lens of the three best and three worst results, it becomes apparent that the model excels when images contain a relatively balanced or significant proportion of the subject, either a cat or dog (reflected by a higher number of '1's in the mask). Conversely, the model tends to underperform in cases where there is a predominance of space relative to the subject in the image (indicated by a higher count of '0's in the mask). This observation suggests that accuracy may not be the most effective metric for measuring performance when there's a stark contrast in the distribution of 'true' pixels (animal present) versus 'false' pixels (no animal). An intriguing avenue for future research would be to develop a model that employs accuracy as a metric when '1's and '0's are present in equal measure and an F1 score for scenarios with an uneven distribution. While the methodology for

such a model is unclear, the concept presents an exciting challenge that warrants further exploration in subsequent projects.

Test Loss:	0.6032233834
Test Accuracy:	0.8651114106
Average Precision:	0.6674499898
Average Recall:	0.3328388262
Average F1 Score:	0.4441782565

The metrics presented in the table provide a multifaceted view of the model's performance on the test dataset. While the test loss of 0.6032 and accuracy of 86.51% suggest that the model is relatively adept at generalizing to new data, the other metrics reveal areas where the model's performance is less than ideal. The average precision of 0.6674 indicates a moderate ability of the model to identify positive examples correctly, but this is not the whole picture. The more telling metrics in this scenario are the average recall and F1 score. With a recall of 0.3328, the model demonstrates a limited capability in identifying all relevant instances; in other words, it misses out on many positive cases. The F1 score, which balances precision and recall, stands at 0.4442, underscoring a weakness in the model's performance, particularly in terms of its harmonized precision and recall. These values collectively suggest a bias in the model's predictions towards adverse outcomes, implying that it predicts 'no animal present' more often than it should. This bias results in many false negatives, where animals present in the image are not being detected. This is detrimental to the model's practical application in scenarios where missing a positive detection could have profound implications. Addressing this imbalance is crucial for enhancing the model's reliability and ensuring it performs well across all relevant metrics, not just loss and accuracy.

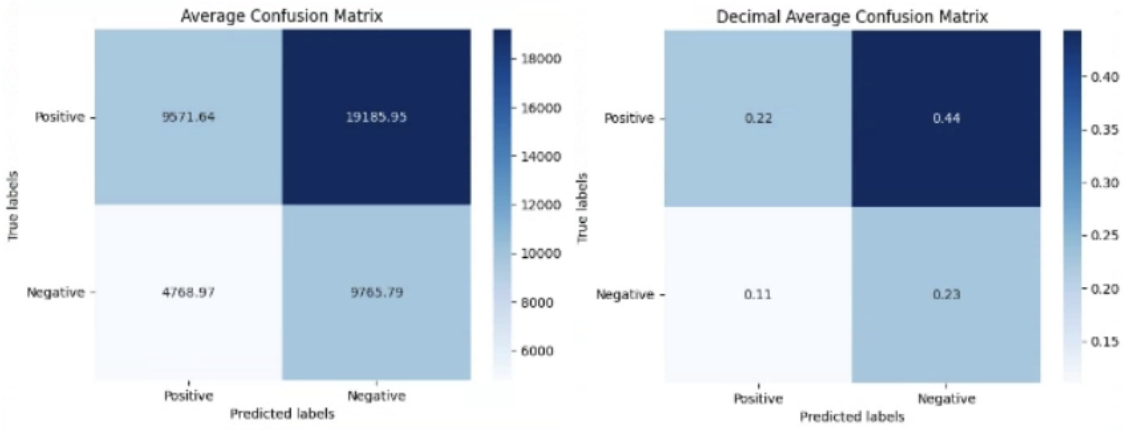

The confusion matrices confirmed the suspicion that the model tends to over-predict negative values. In the first matrix, the number of false negatives is exceptionally high, indicated by the large value in the top right quadrant. The second matrix, presenting decimal average values,

reinforces this assessment. Only 22% of the predictions are true positives, while 44% are false negatives. Furthermore, the proportion of true negatives is twice as large as that of false positives (23% compared to 11%), indicating that the model overestimates negative cases.

Discussion

The model's performance exhibits commendable strengths along with areas ripe for improvement. With a training accuracy reaching approximately 95.06% and a training loss descending to 0.1162, the model demonstrates a robust ability to learn from the training dataset. Validation metrics, while somewhat lower with an accuracy of 86.71% and loss of 0.5849, still suggest that the model generalizes well to new data. When examining the test set, the results provide further insight into the model's efficacy. It achieved a test accuracy of roughly 86.51% and a test loss of 0.6032, which, while aligning closely with the validation metrics, highlight the model's consistent performance on unseen data. However, the training process was halted at 55 epochs due to early stopping, hinting that while the model learned efficiently, it reached a plateau in improvement on the validation set.

Analyzing the three best and three worst predictions reveals insights into the model's limitations, especially in dealing with imbalanced data—images with a higher proportion of the subject versus space. The model's higher performance in the 'best' category, with a more even distribution of 'true' (animal present) versus 'false' (no animal present) pixels, confirms its competence in more balanced scenarios. However, accuracy falls short as a metric for the 'worst' predictions where an uneven distribution skewed towards more empty space led to a disproportionate number of false negatives. This indicates that in imbalanced class distribution cases, other metrics, such as the F1 score, which is sensitive to both precision and recall, offer a more nuanced assessment of model performance.

The confusion matrices underscore this by revealing a notable overestimation of negatives, with false negatives significantly outnumbering the false positives. This imbalance is detrimental, particularly in practical applications where missing an actual positive—failing to detect a present animal—could have significant consequences.

Embracing a cost-sensitive approach is beneficial to bolster the model's performance in future developments. The model would prioritize minimizing these errors by fine-tuning the loss function to impose higher penalties for false negatives, leading to a potentially significant decrease in missed positive detections. In parallel, integrating advanced metrics such as the F1 score, the precision-recall curve, or the area under the precision-recall curve (AUC-PR) into the training feedback loop would enable the model to adjust its learning process in real time to address imbalances effectively. Adjusting the decision threshold could also be a practical tool to balance the precision-recall trade-off, reducing the prevalence of false negatives. Employing ensemble methods may further enhance performance by leveraging the collective strengths of various models, leading to more robust generalizations. Lastly, data augmentation, particularly

for images with uneven class distribution, could give the model a more balanced perspective, training it to recognize and predict minority class features more accurately. These future modifications have the potential to refine the model's predictions, ensuring both its accuracy and reliability are optimized for real-world applications.